Targeting multiple rescatterings through VUV-controlled high-order-harmonic generation

M. R. Miller, C. Hernández-García, A. Jaroń-Becker, and A. Becker

Targeting multiple rescatterings through VUV-controlled high harmonic generation

M. R. Miller,[1, *] C. Hernández-García,[1, 2] A. Jaroń-Becker,[1] and A. Becker[1]

[1] JILA and Department of Physics, University of Colorado, Boulder, CO 80309-0440, USA
[2] Grupo de Investigación en Óptica Extrema, Universidad de Salamanca, E-37008 Salamanca, Spain

We theoretically investigate the use of an isolated attosecond vacuum ultraviolet (VUV) pulse to control the emergence of multiple wavepacket rescatterings in the process of high harmonic generation (HHG). Through numerical solution of the time-dependent Schrödinger equation for a helium atom driven by $0.8 - 2.0$ μm light, we establish the relationship between evidence of multiple rescatterings in HHG and the time delay between the VUV and infrared pulses. We find features of multiple rescatterings present in both the time and frequency domains of emitted HHG, and demonstrate the use of VUV-induced multiple rescatterings for generating trains of ultrashort light pulses.

I. INTRODUCTION

The nonlinear interaction of intense femtosecond lasers with gases yields high-energy coherent light in the form of odd harmonics of the fundamental driving field. The resultant light pulses, emitted with attosecond duration [1–4], can be used to probe and manipulate ultrafast electronic processes [5, 6]. Recent experiments have investigated driving HHG with midinfrared light, and thus extending the harmonic plateau to keV energies [7]. At these longer wavelengths, it has been proposed that electrons which rescatter multiple times from a parent ion play an important role [8], and furthermore may open a way of producing zeptosecond waveforms [9]. However, detection and resolution of light on the zeptosecond time scale as a route to confirm the presence of these multiple rescattering events poses a challenge to current experimental techniques.

As shown previously, interrogation of the process of HHG production can be achieved through the application of a second color of light to the traditional three-step model of HHG [10, 11] (c.f., Fig. 1(a)). Through use of an attosecond pulse train (APT), the excursion distance of an electron wave packet (whether it follows a long or short trajectory to recombine with a specific energy) may be controlled [12, 13]. In the form of an isolated pulse or as an APT, this additional light has been theorized [14, 15] and experimentally demonstrated [16, 17] to enhance the HHG signal. APTs have been used to replace tunnel ionization entirely as a mechanism for electron release, inducing HHG even when the driving laser field strength is insufficient to allow tunnel ionization [18]. And isolated pulses have been studied as a means to filter for and to resolve short and long trajectories on a single-atom scale [19, 20].

In this paper, we investigate an extension of these schemes towards verifying the existence of multiple rescatterings via the control afforded by using an isolated pulse of VUV light. By gating the moment of ionization through the application of the additional light, we

* mrmiller@jila.colorado.edu
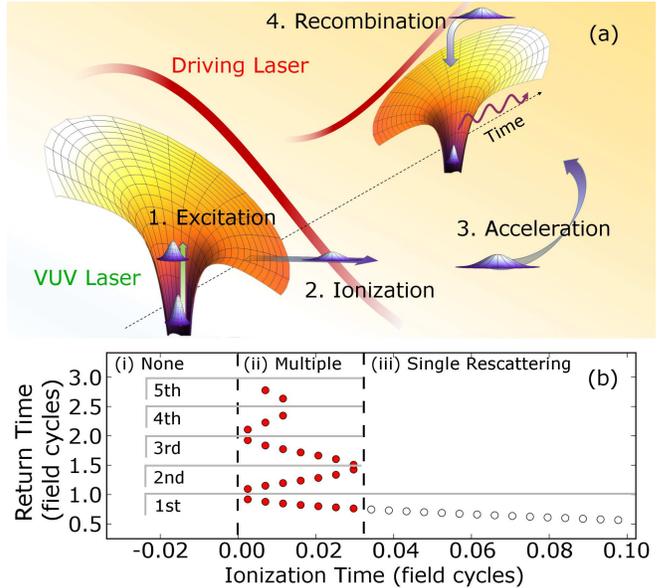
FIG. 1. (Color online) (a) Schematic of the VUV-controlled HHG scheme, in which the moment of ionization is induced by transferring population into excited states using a VUV pulse. Mapping classical predictions of the electron ionization time to return times (b) suggests that multiple rescattering trajectories can be selectively produced in this way.

demonstrate the selective release of electrons into trajectories which revisit the parent nucleus several times and examine the single-atom signatures of multiple rescatterings in both the temporal and frequency domains of the generated radiation. We additionally analyze a way of employing this technique to advance the frontier of ultrashort light pulse production through the use of two VUV pulses.

II. VUV-CONTROLLED HHG SCHEME

In this section we discuss the application of a control scheme based on the gating of electron emission to induce single versus multiple rescattering events. In addition, we

present the methods used for the implementation of the scheme in numerical calculations.

A. Concept

Based on proposals in previous works [12–20], we assert control over the HHG yielded from our system by adding a VUV pulse to interrogate the traditional HHG process (Fig. 1(a)). The target atom, prepared in its ground state, is exposed to an intense infrared (IR) driving laser field. The intensity of this field is tuned to be insufficient for depletion of population from the ground state. An isolated ultrashort VUV light pulse is introduced at a controlled delay time with respect to the IR field, transferring population into excited states that can be depleted by the driving laser. Thus, the transferred population rapidly transitions into the continuum and is propagated in the laser field until recombining with the parent ion and emitting the HHG. In this framework, the time of ionization is gated by the application of the VUV field, so that the time of ionization becomes an accessible and controllable quantity.

The importance of the time of ionization to the multiple rescattering process is readily understood by considering the classical propagation of an electron in a driving laser field [11]. In Fig. 1(b), we consider ionization times throughout one half cycle of the driving field. For each ionization time considered, we then calculate all times of subsequent crossings of zero position. Three separate regimes are evident: (i) an interval of time delays for which no rescattering trajectories are evident, (ii) a second interval generating electrons that rescatter multiple times, and (iii) a third interval of trajectories that will only revisit the parent ion once. Thus, the mediation of ionization via the VUV pulse should lead to control over the production of multiple rescattering trajectories.

B. Calculation methods

We proceed by solving the time-dependent Schrödinger equation (TDSE) for the interaction between a single atom with an external electric field, expressed in Hartree atomic units ($e = \hbar = m = 1$) as

$$i\frac{\partial \Psi(z,\rho;t)}{\partial t} = [H_0(z,\rho) + V_L(t)]\Psi(z,\rho;t), \qquad (1)$$

where H_0 is the field-free Hamiltonian with an effective potential for the helium atom [21] and $V(t) = z\left[E_{IR}(t) + E_{VUV}(t+t_d)\right]$, where $E(t) = E_0 \cos(\omega t)\cos^2(\pi t/\tau)$ for both the IR and VUV fields. In order to retain 2D cylindrical symmetry, we have chosen the linear polarization directions of both the IR and the VUV fields to be parallel. We consider a ten-cycle (full temporal duration, τ_{IR}) IR driving field with peak intensity $I_{IR,0} = |E_{IR,0}|^2 = 1 \times 10^{14}$ W cm^{-2} and $\omega_{IR} = 0.0253$ (wavelength: 1800 nm). At a delay t_d, a

five-cycle VUV field of intensity $I_{VUV,0} = 1 \times 10^{12}$ W cm^{-2} is applied. The frequency is chosen to match the energy gap between the ground and the lowest excited state and, hence, depends on the target atom: for He we choose the 33rd harmonic of the 1800 nm driving field. Throughout the following discussion, time will be considered in units of field cycles of the driving field, with $t = 0$ defined at 4.75 field cycles to coincide with a local field maximum. We have chosen this reference point in time as we will apply the gating VUV pulse either before or after this field maximum.

We have solved the TDSE numerically by using the Crank-Nicholson method on a grid for which z spans from -200 to 200 au and ρ from 0 to 100 au. An absorbing boundary was placed at $z = \pm 180$ au and at $\rho = 90$ au using the exterior complex scaling method [22–25]. The size of this grid, in comparison with the maximum quiver radius of the electron wavepacket in the IR field of 83.4 au, is sufficient to achieve convergence of results. The points were spaced evenly with $\Delta z = 0.1$, $\Delta \rho = 0.2$, and $dt = 0.01$ a.u. The time-dependent wavefunction was used to obtain the HHG radiation spectrum as

$$P(\omega) = \left| \frac{1}{\sqrt{2\pi}} \int_0^T d_{a_z}(t)e^{-i\omega t}dt \right|^2, \qquad (2)$$

where d_{a_z} is the electron dipole acceleration. An inverse Fourier transform over a selected range of frequencies was used to study the yield of the generated attosecond pulses. We further use the continuous wavelet analysis

$$C(t_0,\omega) = \frac{1}{\sqrt{2\pi}} \int_0^T d_{a_z}(t)W\left(\frac{\omega(t-t_0)}{2\pi}\right)dt, \qquad (3)$$

where $W(x) = \frac{1}{\sqrt{\pi}}\exp(2\pi i x)\exp(-x^2)$ is the complex Morlet wavelet.

III. SIGNATURES OF MULTIPLE RESCATTERINGS

To establish our capacity to observe and control multiple rescattering events in HHG, two representative cases are presented and discussed regarding the wavelet analysis, the harmonic spectrum and generation of ultrashort pulses.

A. Wavelet analysis

In Fig. 2(a), the VUV pulse is applied prior to the local maximum of the driving field, at $t_d = -0.065$ field cycles. The wavelet analysis demonstrates a clear signature of multiple reencounters of the wavepacket via the emission of harmonics at every half field cycle subsequent to the initial rescattering. Note that the multiple rescatterings occur despite the application of the VUV pulse at
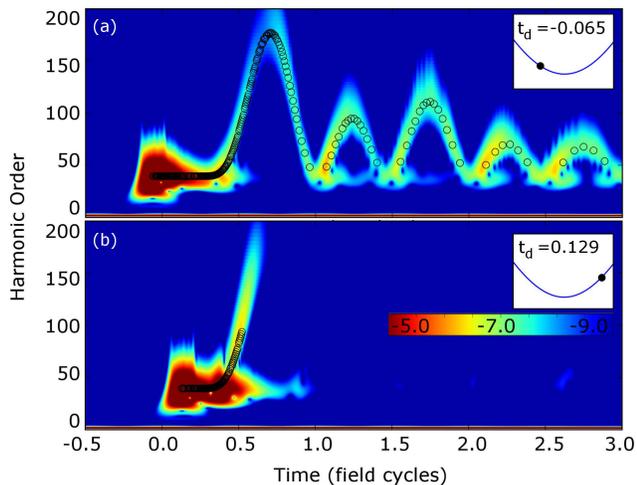
FIG. 2. (Color online) Wavelet analysis of the electron dipole acceleration for application of the VUV pulse at $t_d = -0.065$ (a) and $t_d = 0.129$ (b) field cycles (see inset). Superimposed black circles represent the results of a classical simulation which considers ionization times beginning at the peak of the VUV field and ending at the subsequent zero of the driving field. The presence of several rescattering events in (a) as compared to the single event in (b) shows the desired control. Recombination energies in (b) exceeding the classically predicted energy are attributed to ionization preceding the VUV field maximum.

FIG. 3. (Color online) Harmonic spectra for $t_d = -0.065$ (left) and $t_d = 0.1$ (right). Dashed lines in (a) mark the classically predicted maximum rescattering energies of the first, second, and third events, between which individual subplateaus appear (depicted on linear scale in subpanels). In contrast, (b) lacks subplateaus due to the dominant contribution of an isolated rescattering event. Subpanels, presented on a linear scale, are given in the same arbitrary units as the main panels and, hence, scaled by 10^{-6} to match those of panels (a) and (b).

a time preceding the corresponding interval in our classical analysis (Fig. 1(b)). This is due to the finite width of the VUV pulse and the dispersion of the wavepacket during propagation. The results show that the harmonic emission occurs with similar efficiency at each event. The classically predicted energies of each rescattering event, calculated using ionization times spanning the peak of the VUV field to the subsequent zero of the IR field, are superimposed (black circles) and match well with the results of the quantum mechanical calculation.

These results are contrasted to those in Fig. 2(b), in which the peak of the VUV field is placed at $t_d = 0.129$ field cycles, i.e. after the local field maximum. The dominant contribution to the harmonic emission is observed at the first rescattering event, near $t = 0.5$ optical cycles, without any further significant emission at later times. This is again in agreement with expectations inferred from the classical model, associating this single rescattering event to the recombination of short trajectory electrons. We note as well the participation of these short trajectory events in the previous case of multiple rescatterings: no matter the choice of t_d, sufficient population remains excited through the peak of the driving laser field to generate short trajectory events. This shows that the present scheme allows the isolation of short trajectory events, but not long trajectory events, by choosing an appropriate value of t_d. Nonetheless, our numerical results clearly confirm that selective control over the appearance of multiple rescatterings can be achieved through the ex-

citation of the atom via an ultrashort VUV pulse.

B. High harmonic generation spectrum

Evidence of the multiple rescatterings is present both in the frequency and time domains of the radiated signal (Fig. 3). The HHG spectrum in Fig. 3(a) ($t_d = -0.065$ field cycles) shows a plateau step structure characteristic of multiple rescattering events. The highest harmonic orders (> 110th) are generated in the first rescattering event only ($0.5 < t < 1.0$ field cycles in Fig. 2(a)). The structure in this part of the spectrum results from interference between the so-called short- and long-trajectory contributions. At lower harmonic orders, the HHG spectrum grows in magnitude due to the yields from additional rescattering events and also in complexity due to interferences between events. Both the first and third reencounters of the wavepacket increase yield into energies between $95 - 110$ harmonic orders. Between $70 - 95$ harmonic orders, emission from the first, second, and third rescattering events is present, and so, again, the overall yield is seen to increase, comprising another subplateau. Emission of harmonics below the 70th harmonic order occurs throughout all rescattering events, and thus constitutes another final increase in the overall harmonic yield.

In contrast, for a single rescattering event the resultant HHG plateau shows little interference structure (Fig. 3(b)), as photons at each harmonic order are emitted at only one time instant (see Fig. 2(b)). Furthermore, there is no evidence of subplateaus throughout the plateau. From this, we conclude that the appearance of subplateaus within the HHG plateau may be used to ex-
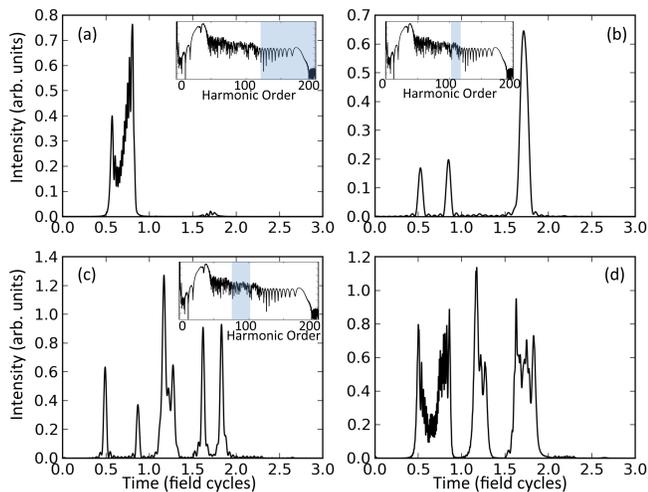
FIG. 4. (Color online) Attosecond pulse formation for $t_d = -0.065$, constructed by transforming energies corresponding to each of the subplateaus distinguished in Fig. 3: in (a), $115-180$ harmonic orders; in (b), $100-115$ harmonic orders; in (c), $75-100$ harmonic orders; and in (d), $75-180$ harmonic orders, comprising the full HHG plateau. The inset figure is reproduced from Fig. 3(a), with shaded regions corresponding to the energies considered.

perimentally identify the presence or absence of multiple rescattering events as the VUV delay time is changed. We expect that the subplateaus will become even more apparent for driving laser fields of greater wavelength or intensity than modeled in this study, as increasing either parameter will also increase the difference between the maximal energies achieved by each rescattering event.

C. Attosecond pulse generation

The existence of multiple rescattering events is further evidenced by examining harmonic emission in the time domain. In Fig. 4, we consider the temporal signature of multiple rescatterings induced by placing the VUV field at $t_d = -0.065$. By considering each of the subplateaus identified in Fig. 3, we connect the appearance of individual pulses within the full pulse train (Fig. 4(d)) to separate rescattering events. Beginning in Fig. 4(a), we select energies contributing only to the highest-energy subplateau. As indicated by Fig. 2(a), these energies contribute exclusively to the first rescattering of the electron wavepacket, and thus lead to the formation of an isolated attosecond pulse located between $0.5-1.0$ field cycles in Fig. 4(a). Similar examination of the next subplateau with energies spanning 100-115 harmonic orders leads to the appearance of a new pulse between $1.5-2.0$ field cycles, representing the participation of the third rescattering event. Likewise, transformation of energies between $75-100$ harmonic orders constructs an additional pulse between $1.0-1.5$ field cycles due to yield from the second
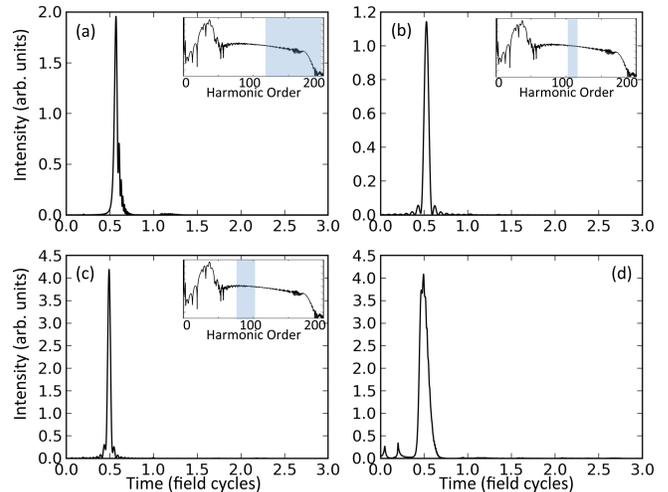
FIG. 5. (Color online) Attosecond pulse formation for $t_d = 0.1$, with subpanels considering transformations of the same energy values as Fig. 4. Each subpanel reproduces an isolated attosecond pulse corresponding to the single emission event allowed by the placement of the VUV field. The inset figure is reproduced from Fig. 3(b).

rescattering event. The full temporal picture of the HHG spectrum, considered in Fig. 4(d), thus forms an attosecond pulse train which can be used as a clear signature of multiple rescatterings in the temporal domain.

In Fig. 5 we consider instead the temporal signature of an electron wavepacket which rescatters by centering the VUV field at $t_d = 0.1$ field cycles. Considering the same energy ranges as in the previous analysis in Figs. 5(a)-(c), we construct in each case an isolated attosecond pulse occurring between $0.5-1.0$ field cycles. The suppression of radiation outside of this time interval is caused by the elimination of high-order rescattering events, so that each energy regime receives yield only during the first rescattering. The temporal width and position of the pulse is related to, and thus varies with, the time of emission of the energies it contains. Consequently, the pulse containing the largest bandwidth (corresponding to the longest time interval of emission) has the greatest temporal width. This feature is most evident in Fig. 5(d), for which transformation of the complete HHG temporal signal shown in Fig. 5(d) is an isolated attosecond pulse.

IV. DEPENDENCE ON DRIVING LASER WAVELENGTH

We now examine how the control strategy generalizes for the resolution of multiple rescattering events using different driving field wavelengths. In Fig. 6 we consider driving HHG using wavelengths of 0.8, 1.2, and 2 μm. In each case, the VUV field is centered at $t_d = -0.08$ field cycles, before the local field maxima and consequently gating for multiple rescattering events. The duration of
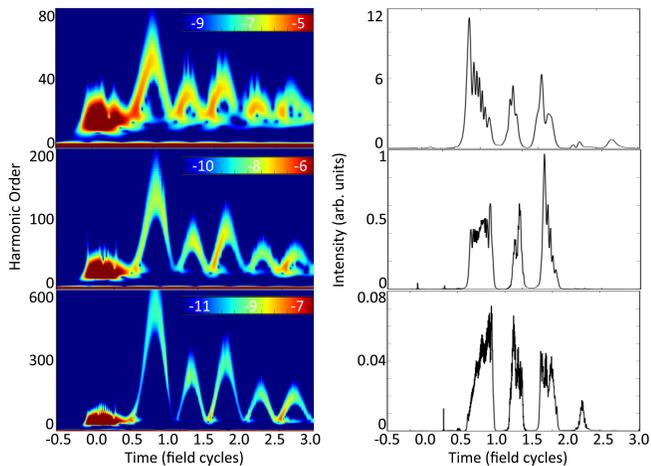
FIG. 6. (Color online) In the first column, the time-frequency analysis of the HHG spectrum driven by the combination of an IR laser pulse (intensity 2.5×10^{14} W/cm^2) and a VUV field: in the first row, 0.8 μm (9.6 fs FWHM) IR and 6 cycles full width (392 as FWHM) VUV; in the second row, 1.2 μm (14.4 fs FWHM) IR and 9 cycles (589 as FWHM) VUV; in the third row, 2 μm (24 fs FWHM) IR and 15 cycles (981 as FWHM VUV. In each case, the VUV field is centered at -0.08 field cycles. In the second column, the temporal profile of harmonics with energies exceeding 2.2 au is shown for each driving wavelength.

FIG. 7. (Color online) (a) Time evolution of the frequency emission due to the application of two VUV pulses at $t_d = -0.53$ and $t_d = -0.03$ field cycles. Superimposed are classical predictions induced by the first (black circles) and the second (white circles) VUV pulse. The harmonic spectrum (b) is structurally similar to the case of multiple rescatterings shown in Fig. 3 (a), but exhibits additional interference. The intensity profile of the radiation is shown in (c), in which every element of the attosecond pulse train with the exception of the first demonstrates a substructure beating; (d) examines this substructure between 0.5 and 1.0 field cycles.

this pulse is scaled to persist for the same fraction of a field cycle for each driving wavelength to liberate electrons that follow similar trajectories in each case. We also consider an increased field intensity of 2.5×10^{14} W/cm^2, which remains weak enough to suppress significant ionization from the ground state relative to the population transferred by the VUV field.

The time-frequency analyses performed in Fig. 6 demonstrates that multiple rescattering events are generated similarly in each case. In the conventional (one pulse) scenario of HHG, including the release of electron wavepackets at every half field cycle, short driving wavelengths pose a particular challenge for multiple rescattering resolution due to the decreased energy separation between coincident rescattering events. As the present control scheme enables the isolated release of a single electron wavepacket, it is possible to resolve each rescattering event in the wavelet analysis (upper row), even at the shortest driving wavelength. This clearly corresponds to the separation of each rescattering event in the temporal domain, as seen in the second row of Fig. 6. Here, for each wavelength, we observe the formation of well-defined attosecond pulse trains, where each pulse within the train again corresponds to a different rescattering order.

V. PRODUCTION OF ULTRASHORT LIGHT PULSES WITH TWO VUV FIELDS

Finally, we examine the possibility of applying more than one VUV pulse to yield ultrashort light pulses. To investigate this scenario, we apply two isolated VUV pulses of same peak intensity and wavelength at delay times spaced one half cycle of the driving 1.8 μm IR field apart in time, at $t_d = -0.53$ and $t_d = -0.03$ field cycles. The wavelet analysis of the resulting dipole acceleration in Fig. 7(a) demonstrates two separate sets of multiple rescattering events in agreement with the classical predictions for ionization induced at each of these delay times. Reencounters of the wavepackets with the parent ion occur simultaneously for times following 0.5 field cycles. However, the energies emitted by the respective wavepackets are distinct at each event. Evidence of two multiple rescattering wavepackets is contained within the resulting harmonic signal of Fig. 7(b). Subplateaus are evident, substantiating multiple revisitations; however, we further note another signature of the presence of two rescattering wavepackets, namely that even harmonic orders are now emitted even throughout the highest energies of the plateau. Instances of coincident rescatterings are apparent in the temporal structure of the emitted radiation as well, shown in Fig. 7(c) for harmonics in excess of the 75th order. The pulse train profile, characteristic of multiple rescatterings, is now modulated by a rapidly beating substructure for all but the first pulse of

the train. In the second pulse, shown in Fig. 7(d), this beating occurs with a period of $\tau \approx 3.0$ au, corresponding to an energy of 80 harmonic orders of the driving field which matches the classically predicted energy difference between photons emitted by simultaneously rescattering wavepackets. This difference is proportional to the ponderomotive energy, U_p, so that increasing either the wavelength or intensity of the driving field will decrease τ.

VI. CONCLUSIONS

We have demonstrated the use of isolated attosecond VUV pulses to target the formation and detection of multiple rescattering trajectories on the single atom level. Gating the moment of ionization with a VUV pulse has been shown to provide conclusive signatures of multiple rescatterings both in the frequency and time domains. Furthermore, the capacity to target multiple wavepacket rescatterings in the HHG process may allow for their further use as experimental tools; for example, in the modulation of ultrashort laser pulses.

[1] I.P. Christov, M.M. Murnane, and H.C. Kapteyn, Phys. Rev. Lett. **78**, 1251 (1997).

[2] P.M. Paul, E. S. Toma, P. Breger, G. Mullot, F. Auge, P. Balcou, H. G. Muller, and P. Agostini, Science **292**, 1689 (2001).

[3] E. Goulielmakis, M. Schultze, M. Hofstetter, V. S. Yakovlev, J. Gagnon, M. Uiberacker, A. L. Aquila, E. M. Gullikson, D. T. Attwood, R. Kienberger, F. Krausz, and U. Kleineberg, Science **320**, 1614 (2008).

[4] K. Zhao, Q. Zhang, M. Chini, Y. Wu, X. Wang, and Z. Chang, Opt. Lett. **37**, 3891 (2012).

[5] T. Popmintchev, M.-C. Chen, P. Arpin, M.M. Murnane, and H.C. Kapteyn, Nat. Photonics **4**, 822 (2010).

[6] P. B. Corkum and F. Krausz, Nat. Phys. **3**, 381 (2007).

[7] T. Popmintchev, M.-C. Chen, D. Popmintchev, P. Arpin, S. Brown, S. Ališauskas, G. Andriukaitis, Tadas Balčiunas, O. D. Mücke, A. Pugzlys, A. Baltuška, B. Shim, S. E. Schrauth, A. Gaeta, C. Hernández-García, L. Plaja, A. Becker, A. Jaron-Becker, M. M. Murnane, and H. C. Kapteyn, Science **336**, 1287 (2012).

[8] J. Tate, T. Auguste, H. G. Muller, P. Salières, P. Agostini, and L.F. DiMauro, Phys. Rev. Lett. **98**, 013901 (2007).

[9] C. Hernández-García, J. A. Pérez-Hernández, T. Popmintchev, M. M. Murnane, H. C. Kapteyn, A. Jaron-Becker, A. Becker, and L. Plaja, Phys. Rev. Lett. **111**, 033002 (2013).

[10] K. J. Schafer, B. Yang, L. F. DiMauro, and K. C. Kulander, Phys. Rev. Lett. **70**, 1599 (1993).

[11] P. B. Corkum, Phys. Rev. Lett. **71**, 1994 (1993).

[12] K. J. Schafer, M. B. Gaarde, A. Heinrich, J. Biegert, and U. Keller, Phys. Rev. Lett., **92(2)**, 023003 (2004).

[13] C. Figueira de Morisson Faria, P. Salières, P. Villain, and M. Lewenstein, Phys Rev A **74(5)**, 053416 (2006).

[14] A. D. Bandrauk, S. Chelkowski, and H.S. Nguyen, App. Phys. B **77**, 337 (2003).

[15] K. Ishikawa, Phys. Rev. Lett. **91**, 043002 (2003).

[16] A. Heinrich, W. Kornelis, M. P. Anscombe, C. P. Hauri, P. Schlup, J. Biegert, and U. Keller, J. Phys. B **39**, S275 (2006).

[17] F. Brizuela, C.M. Heyl, P. Rudawski, D. Kroon, L. Rading, J.M. Dahlström, and A. L'Huillier, Scientific Reports, **3**, 1410 (2013).

[18] G. Gademann, F. Kelkensberg, W.K. Siu, P. Johnsson, M.B. Gaarde, K.J. Schafer, and M.J.J. Vrakking, New Journal of Physics, **13(3)**, 033002 (2011).

[19] P. Lan, P. Lu, W. Cao, and X. Wang, Phys. Rev. A **76**, 043808 (2007).

[20] S.-F. Zhao, X.-X Zhou, P.-C. Li, and Z. Chen, Phys. Rev. A, **78**, 063404 (2008).

[21] X. M. Tong, and C. D. Lin, J. Phys. B **38**, 2593 (2005).

[22] F. He, C. Ruiz, and A. Becker, Phys. Rev. A **75**, 053407 (2007).

[23] C. W. McCurdy, M. Baertschy, and T. N. Rescigno, J. Phys. B **37**, R137 (2004).

[24] L. Tao, W. Vanroose, B. Reps, T. N. Rescigno, and C. W. McCurdy, Phys. Rev. A, **80**, 063419 (2009).

[25] A. Scrinzi, Phys. Rev. A **81**, 053845 (2010).